Control of size, fate and time by the Hh morphogen in the eyes of flies

David G. Miguez [a,*], Diana Garcia-Morales [b], Fernando Casares [b,*]

[a] Dept. Física de la Materia Condensada, Instituto de Física de la Materia Condensada (IFIMAC), Facultad de Ciencias, and Centro de Biología Molecular Severo Ochoa (CBMSO, CSIC-UAM), Universidad Autónoma de Madrid, Madrid, Spain
[b] CABD (Andalusian Centre for Developmental Biology), GEM-DMC2 Maria de Maeztu Unit, CSIC-Universidad Pablo de Olavide-Junta de Andalucia, Campus UPO, Seville, Spain
* Corresponding authors: *Email addresses:* david.miguez@uam.es (D.G. Miguez); fcasfer@upo.es (F. Casares)

Contents

Abstract

Molecules of the *hedgehog* (*hh*) family are involved in the specification and patterning of eyes in vertebrates and invertebrates. These organs, though, are of very different sizes, raising the question of how Hh molecules operate at such different scales. In this paper we discuss the strategies used by Hh to control the development of the two eye types in *Drosophila:* the large compound eye and the small ocellus. We first describe the distinct ways in which these two eyes develop and the evidence for the key role played by Hh in both; then we consider the potential for variation in the

Current Topics in Developmental Biology, Volume xx
ISSN 0070-2153, https://doi.org/10.1016/bs.ctdb.2019.10.011

range of action of a "typical" morphogen and measure this range ("characteristic length") for Hh in different organs, including the compound eye and the ocellus. Finally, we describe how different feedback mechanisms are used to extend the Hh range of action to pattern the large and even the small eye. In the ocellus, the basic Hh signaling pathway adds to its dynamics the attenuation of its receptor as cell differentiate. This sole regulatory change can result in the decoding of the Hh gradient by receiving cells as a wave of constant speed. Therefore, in the fly ocellus, the Hh morphogen adds to its spatial patterning role a novel one: patterning along a time axis.

1. THE SMALL AND LARGE EYES IN *DROSOPHILA* RELY ON HH

Insects typically harbor two eye types. Two large compound eyes (CE), located laterally, and three small eyes, called ocelli (OC), on the dorsal medial head—the so-called ocellar complex (Fig. 1A). CEs are the main visual organs, responsible for color and motion vision and the detection of polarized light. OC might have different functions in different insect species, but they have been generally involved in the detection of fast changes in light intensity, such as those produced by looming objects, to trigger a fast escape reflex, or helping in the detection of the horizon during flight (Krapp, 2009). CEs and OC are of very different sizes. In *Drosophila*, each CE comprises about 16,000 cells (of which 6400 are photoreceptors ("PR") cells), while each of the three OC is formed by about 80 cells (with 40 PRs each). However, and despite their very different size and structure (the CE is formed by many small unit eyes, called ommatidia, while each CO is a single retina), their genetic makeup is very similar (Blanco, Pauli, Seimiya, Udolph, & Gehring, 2010; Brockmann, Dominguez-Cejudo, Amore, & Casares, 2011; Friedrich, 2006).

Both eyes types derive from two bilateral head primordia (also called "eye-antennal imaginal discs"; Fig. 1B; Haynie & Bryant, 1986) which fuse during the fly's metamorphosis to give rise to most of the fly head, including its major sensory organs (in addition to the CEs and OC, the antenna and the maxillary palps (the olfactory and gustatory organs, respectively) also derive from the same primordium). The eye-antennal disc is a monolayer epithelium, and in it, each organ has its own Hh source (Fig. 1B). Specifically, prior to the differentiation onset, Hh is expressed along the disc's margin in two regions: posterior, for the CE (Borod & Heberlein, 1998; Bras-Pereira, Bessa, & Casares,

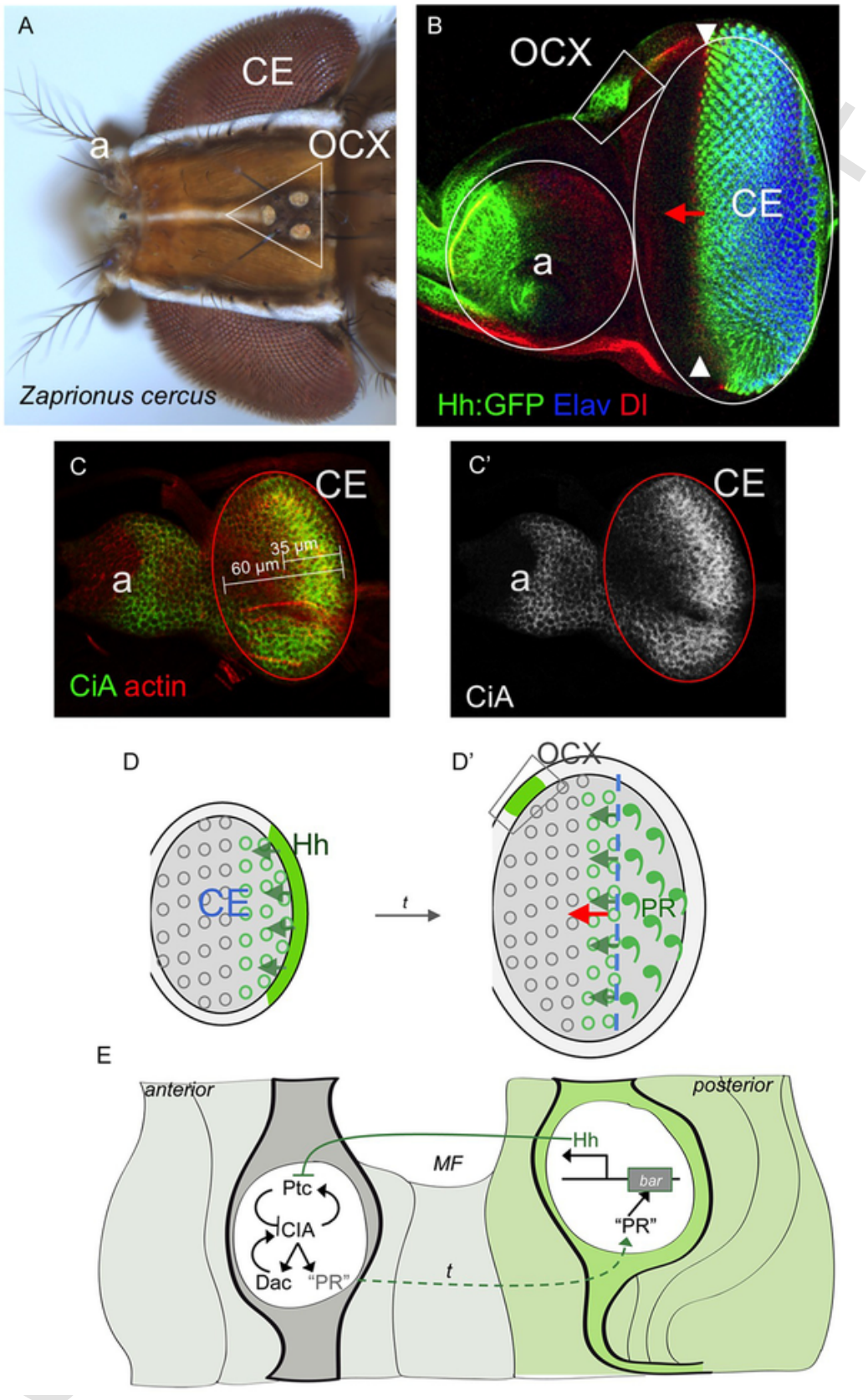

Fig. 1. (A) Dorsal view of *Zaprionus cercus* (NHMUK010579619) head showing the visual organs typical of a fly: the large lateral compound eyes (CEs) and the three dorsal ocelli, arranged in a triangle—the ocellar complex (OCX). The antennae ("a") develop in

the frontal head. (B) The head primordium or "eye imaginal disc" of a Hh:GFP *Drosophila melanogaster* larva. The expression of GFP-tagged Hh is driven from a BAC that recapitulates endogenous *hh* expression. The prospective antenna, CE and OCX regions are marked. The primordium has been stained for Hh (GFP, green), the photoreceptor marker Elav (blue) and the *Notch* ligand *Delta* (*Dl*), which is used here to outline the different disc's regions. The two arrowheads mark the position of the differentiation wave-front (the so-called "morphogenetic furrow," or MF). (C,C′) Before the onset of PR differentiation, Hh produced at the posterior margin signals across a domain 30–40 μm wide, when the width of the primordium is about 60 μm. Hh signaling readout is CiA (the activator form of *cubitus interruptus*, *ci*). The disc has been counterstained with rhodamine phalloidin ("actin") to outline the tissue. CiA and actin signals (C) or only CiA (C′) are shown. (D) Initiation of PR differentiation depends on Hh produced at the primordium's posterior margin. Once differentiation starts (D′), PRs (inverted comas) express Hh themselves, causing a positive feedback that drives the movement of the differentiation wave across the primordium. Only when the CE differentiation is midway the differentiation of the OCX region starts. (E) Schematic representation of the Hh feedforward signaling. In the retina precursor cells Hh binds to Ptc, blocking its repressing action on the pathway. As a consequence, CiA accumulates and activates the expression of target genes. Among these targets is Ptc itself. In the CE the nuclear factor *dachshund* (Dac) is required for full pathway activation (Bras-Pereira et al., 2016). Downstream of the signaling the photoreceptor differentiation pathway ("PR") is activated. With time, this pathway is expressed and the PR cells differentiate. As part of this differentiation program, PR cells activate the expression of Hh through a retina-specific enhancer, *bar3*. The transition from precursor cells to PRs happens as cells constrict transiently (MF). The direction of differentiation is marked with a red arrow (in B, D′). See text for references.

2006; Dominguez & Hafen, 1997) and dorsal, for the OC (Aguilar-Hidalgo et al., 2013; Blanco, Seimiya, Pauli, Reichert, & Gehring, 2009; Dominguez-Cejudo & Casares, 2015; Royet & Finkelstein, 1996).

This early Hh expression is necessary for the onset of retina differentiation in both eyes (Dominguez & Hafen, 1997; Ma, Zhou, Beachy, & Moses, 1993; Royet & Finkelstein, 1996). Beyond flies, the role of Hh-family morphogens in retina development is conserved in vertebrates (Neumann & Nuesslein-Volhard, 2000), which also exhibit a huge range of eye sizes in different species. Therefore, the two *Drosophila* Hh-controlled eyes, with similar genetics but very different size, represent an excellent system to explore how the Hh patterning mechanisms cope with these spatial scale differences.

2. THE RANGE OF HH ACTION IS SMALL AND CONSTANT IN DIFFERENT ORGANS

The onset of retina differentiation in the CE happens after the transition from the second to the third (and last) larval instar (L3). At this point, the width of the retina progenitor field is about 60 μm (Fig. 1C). The differentiation of the OC starts later, in mid-L3, and the width of the ocellar field is also about 50 μm (Garcia-Morales et al., 2019). Therefore, and with a cell diameter of 4–5 μm, the Hh signaling sources have a field of 10–15 cell wide ahead of them at the onset of differentiation.

We have measured the characteristic length of the Hh gradient (the length from the source at which the gradient reaches 1/*e* of its maximal amplitude and which gives an intuitive idea of the gradient's range), using a transgenic BAC that drives expression of a GFP-tagged Hh within its normal expression domains and at functional levels (Chen, Huang, Hatori, & Kornberg, 2017). The Hh's characteristic length is about constant in different organs (11–14 μm; Fig. 2). The range of action of the signaling pathway in receiving cells of the CE, monitored by the accumulation of the activator form of the Gli TF *ci*, CiA (Alexandre, Jacinto, & Ingham, 1996; Dominguez, Brunner, Hafen, & Basler, 1996), is about 30–40 μm (Fig. 1C). These ranges are definitely too short to explain a Hh-mediated differentiation of the CE, with a final width of more than 200 μm (Vollmer et al., 2016).

3. A HH-DRIVEN POSITIVE FEEDBACK LOOP INDUCES A DIFFERENTIATION WAVE ACROSS THE DEVELOPING CE

In *Drosophila*, the adult CE comprises about 16,000 cells, but some fly species (including common species such as house flies, hoverflies or horse flies) harbor eyes several times larger (in cell number). It is the vigorous proliferation of the eye's progenitor cells that drives the growth of the CE (reviewed in Amore & Casares, 2010; Casares & Almudi, 2016). Hh produced from the posterior center triggers the expression of *ato* (transforming the progenitors into retina precursors) and

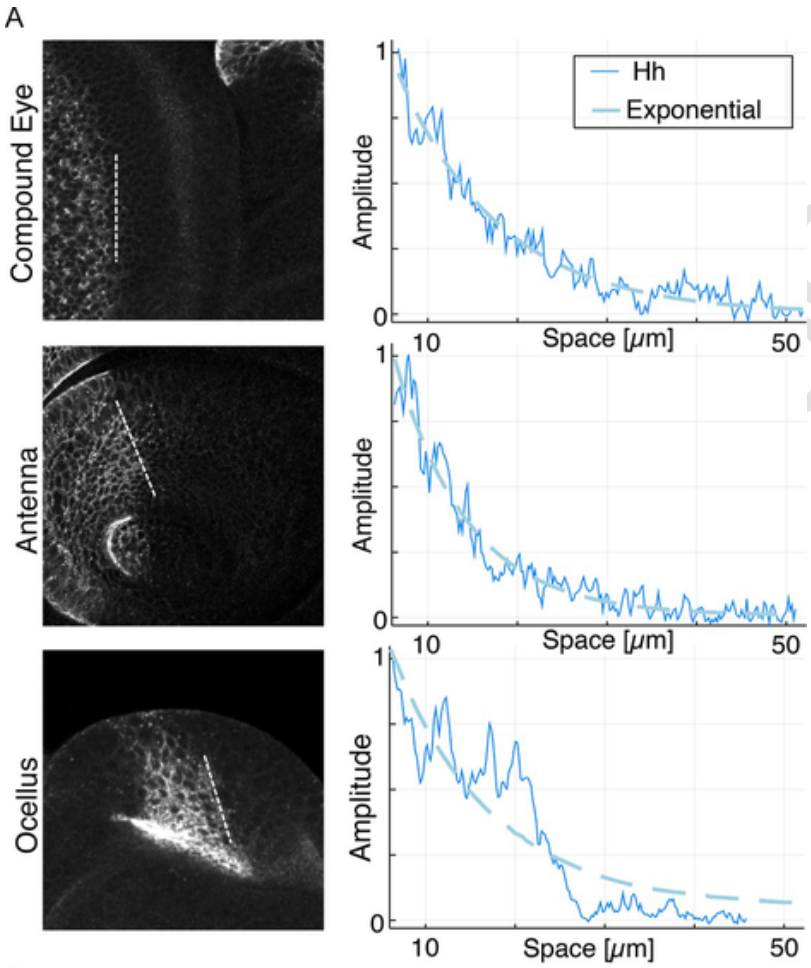

Fig. 2. Characteristic length of the Hh gradient. (A) Expression of GFP:Hh in different organs (left column) and its quantitative distribution (right). This distribution fits an exponential gradient. The characteristic length is similar in the three organs shown, including the compound eye (CE) and ocellus (OC) and about 12–15 μm.

the ensuing differentiation of the first PR cells of the retina (Dominguez, 1999). These PRs (and some accessory cells) cluster in regular cellular arrays, the future ommatidia. Within each ommatidium,

of the eight PRs cells (R1–8), all but R8 express Hh (Rogers et al., 2005). Therefore, with each new row of ommatidia that is added to the retina, the front of the Hh source moves forward, recruiting further progenitors into differentiating ommatidia, so that the moving differentiating wave sweeps across the primordium until no further progenitors are left and the eye reaches its final size (Fig. 1D and E; Fried et al., 2016; Treisman, 2013). Therefore, the positive feedback loop "Hh recruits PRs that produce more Hh" makes the differentiation wave-front move forward. At the wave-front, cells transiently constrict, generating a characteristic "furrow" (the so-called "morphogenetic furrow," or "MF," as it is associated to the initiation of cell differentiation and assembly into ommatidia). The regulatory mechanism enabling the positive feedback has been elucidated. A *hh* CE-specific enhancer (*hhbar3*) is activated in R1–7 PRs (Pauli, Seimiya, Blanco, & Gehring, 2005; Rogers et al., 2005) (by EGF signaling, with the Ets transcription factor Pointed (Pnt) (Rogers et al., 2005) and the Six2 transcription factor Sine-oculis (So) (Pauli et al., 2005) directly binding and activating this enhancer) (Fig. 1E). In mutants in which the *hhbar3* enhancer is deleted, only the posterior *hh* source contributes to retinogenesis and, in the absence of the self-propagating wave, the mutant eye is only a sixth of the normal one (Rogers et al., 2005).

A Hh-driven wave as a mechanism to pattern a large organ is also used during the patterning of the retina in vertebrates (Viets, Eldred, & Johnston, 2016). But in principle, there are alternative strategies for a morphogen to pattern a large organ. For example, in the case of the neural tube in amniotes, dorso-ventral (DV) patterning occurs in two phases: first, Shh (aided by antiparallel signaling gradients of Wnt and BMP molecules) establishes a number of adjacent domains along the DV axis within its range of action, and then, once the pattern has been established, the organ grows and the pattern scales to sizes beyond Shh's range (reviewed in Kicheva & Briscoe, 2015). However, we note that these two patterning mechanisms differ substantially: while patterning and growth of the neural tube represent two functionally distinct phases in time, in the retina patterning and growth occur *simultaneously*. The patterning role of Hh in the neural tube is essentially spatial, while in the retina it is temporal. In this latter, the polarized expression of Hh links the paced recruitment of PRs to space, so that succes-

sive recruitment steps in time are also successive in space, generating a wave.

The Hh-driven wave not only allows for patterning a larger organ, but can also influence the final organ's size (Fried et al., 2016). For example, increasing the velocity of the wave (relative to the growth rate of the progenitors) may result in a smaller CE, as the wave would exhaust the progenitor pool faster. The regulation of the velocity of wave movement is controlled by Hh signaling (Fu & Baker, 2003; Greenwood & Struhl, 1999) and can be modulated by genes regulating the intensity of Hh signaling (Baker, Bhattacharya, & Firth, 2009; Bras-Pereira et al., 2016; Zhang et al., 2006). Also, the movement of the wave involves a number of processes (tissue furrowing, cell cycle synchronization, proneural gene activation, etc.), mostly mediated by Hh-regulated gene expression, that might suggest the need for a mechanism coordinating them all. However, this may not be necessary. The Hh-driven wave is built in a way that is "biochemically coupled." That is, by making the production of Hh dependent upon PR differentiation, which is itself Hh dependent, the velocity of differentiation is exactly the time that Hh-receiving cells take to differentiate and re-initiate Hh production. For example, in *dachshund* (*dac*) mutant cells Hh signaling is weakened (Bras-Pereira et al., 2016), and this results in the global slowing down of the differentiation wave, not in a desynchronization of the individual processes. This fact might allow the system to easily accommodate variations in biochemical rates, like those produced, for example, by temperature fluctuations, without affecting the process significantly.

4. HH SETS THE STAGE FOR OCELLUS DEVELOPMENT

The three ocelli are the small eyes. After the OC complex region has been specified, a process in which Hh also plays a major role (Dominguez-Cejudo & Casares, 2015; Royet & Finkelstein, 1996), Hh is expressed in a small domain (Fig. 3A). From this domain, Hh induces the expression of retinal determination genes (Eya and its partner So/Six2) in two retina-competence domains: one posterior (p) and another anterior (a) which will give rise to one posterior ocellus (pOC) and half of the anterior ocellus (aOC), respectively (the left and right

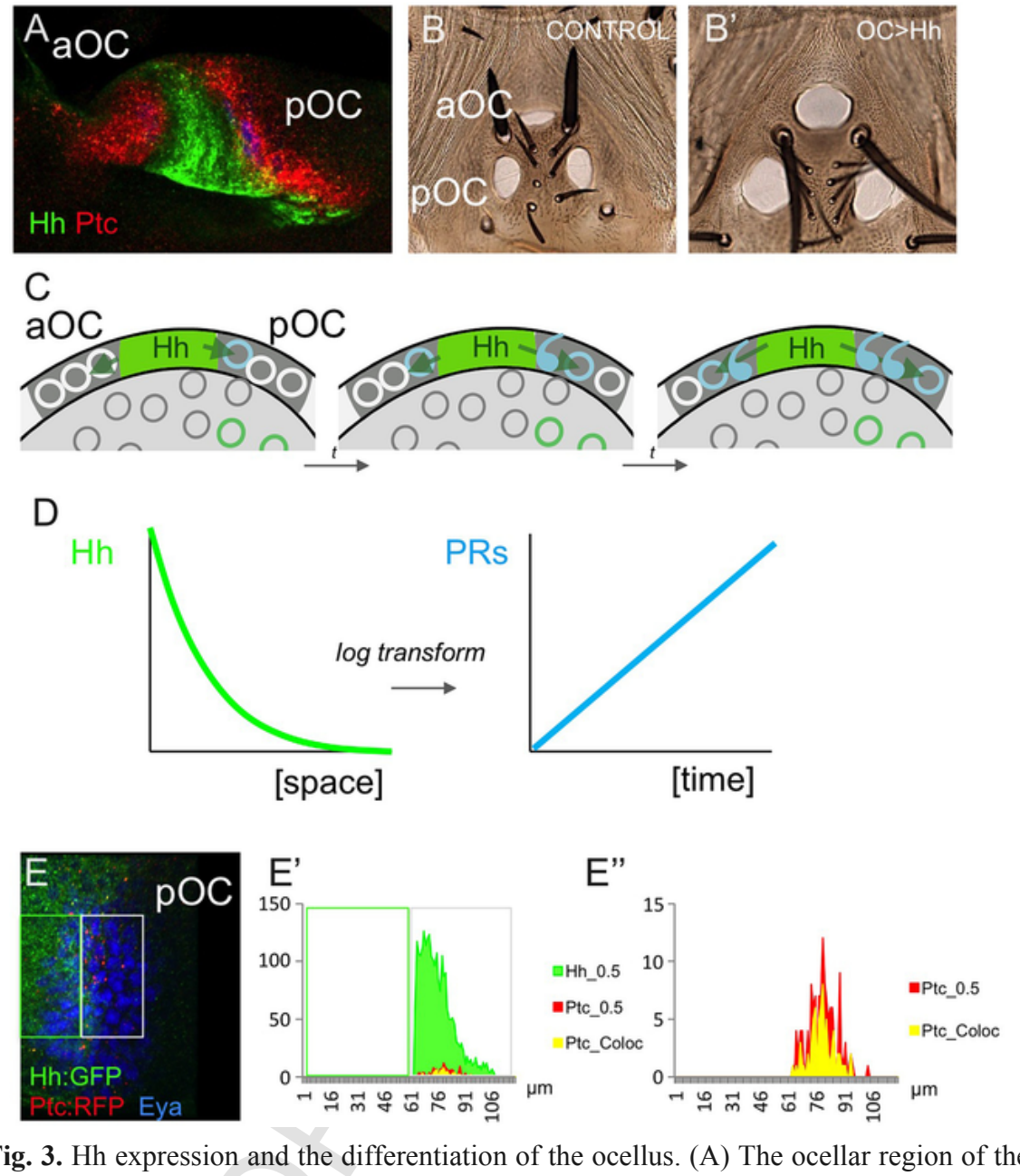

Fig. 3. Hh expression and the differentiation of the ocellus. (A) The ocellar region of the head primordium has one Hh-producing domain (green) that signals to two adjacent domains. These domains, which upregulate the expression of the Hh receptor Ptc will give rise to the posterior ocellus (pOC) and half of the anterior ocellus (aOC). The two head primordia fuse during metamorphosis to give rise to two pOC and one aOC, that results from the merging of the left and right halves (B). (B) View from the top of the ocellar region. The lenses are visible. Underneath these lenses lie the retinas. When Hh is overproduced in the OC primordia, the size of the resulting OCs is dramatically increased (B′, "OC > Hh"). (C) The differentiation of the ocellar retinas proceeds as a wave, with the differentiation of the aOC lagging behind the pOC. Upon receiving the Hh signal, OC primordium cells (white circles) activate the expression of proneural genes (cyan circles) to then differentiate (cyan comas). This differentiation proceeds as a wave, starting close to the Hh source (green) and moving away progressively. (D) A non-linearly decaying signal across the OC primordium is transformed into a differentiation wave of constant

speed. Degree of colocalization of the fluorescently tagged forms of Hh (Hh:GFP, green) and Ptc (Ptc:RFP, red) in the pOC (co-stained for Eya, which marks the extent of the retina competent region, E). Most of Ptc is colocalized with Hh (represented in yellow) and the ratio of Ptc bound to Hh ("Ptc_Coloc," yellow) to total Ptc ("Ptc_0,5," red) is about constant across all the competence domain (E′,E″). In (E″) the Ptc and Ptc:Hh signal is shown.

parts of the fly body derive from paired imaginal discs. The two half aOCs meet at the head midline to form the anterior single ocellus when the two discs fuse during metamorphosis) (Aguilar-Hidalgo, Casares, & Lemos, 2018; Aguilar-Hidalgo et al., 2013; Blanco et al., 2009). The aOC domain is smaller and its differentiation starts later than the pOC. Since both anterior and posterior OC depend on Hh for their development (and the aOC readily responds to increased Hh signaling by increasing dramatically its size (Fig. 3A and B)) signaling differences must exist, either in the quantity or the quality of the signal itself or in the "perception" of the signal between the anterior and posterior OCs that account for this different response. In fact, only the aOC expresses the Six3 transcription factor *optix* (Dominguez-Cejudo & Casares, 2015) indicating that, although very similar in morphology, the genetic makeup of both ocelli is distinct (Dominguez-Cejudo & Casares, 2015; Maynard-Smith & Sondhi, 1960). Still, it is not clear how this difference translates into differential Hh signaling.

5. THE OCELLUS, THE SMALL EYE, IS PERHAPS STILL TOO LARGE FOR HH

Once the two ocellar domains have been genetically defined, Hh has the task of controlling the differentiation of these small retinas. The pOC is about 50 μm across (10–12 cells), and gives rise to a total of about 80 cells, of which 40 are photoreceptor neurons. In contrast with the CE, that comprises PR cells of several types, all OC PRs express rhodopsin 2 and therefore are likely of a single type (Mismer, Michael, Laverty, & Rubin, 1988). Ocellar PR differentiation has been described in detail and shown to proceed as a wave of constant speed (Garcia-Morales et al., 2019; Fig. 3C). The first PRs to differentiate are those close to the Hh source and then differentiation proceeds sequentially farther away. This is reminiscent of the CE differentiation wave. An obvious driving mechanism for this wave would be, again, that OC PRs

expressed Hh as they differentiate, but this is not the case (Garcia-Morales et al., 2019). Another option is that the signaling gradient is capable of controlling the wave without self-propagation. However, the typical characteristic length of the Hh gradient at this time point is about 15 μm (Fig. 2), that is, three to four cells. This means that the cells closer to the source would be much more exposed to the signal than cells a bit farther apart. If the probability of a cell to differentiate is proportional to the level of (accumulated) Hh signaling (Dessaud et al., 2007), this would result in a non-linear pattern of differentiation—in contrast to what is observed (Fig. 3D and Garcia-Morales et al., 2019). In addition, with very sharp gradients, the effective range of action of the signaling gradient may be too short even to induce differentiation across the whole width of the ocellus. Are there ways for a Hh gradient to signal farther away?

6. STRETCHING AND LINEARIZING A GRADIENT

At this point we will introduce the mathematical description of a gradient to explore mechanisms that may extend its reach. To simplify the equations, we will replace Hh, the ligand, by "*u*," and its receptor (mainly representing Ptc) by "*v*" (Box 1). In a typical morphogen gradient, the morphogen *u* is produced and secreted at a specific domain ("source") from which it spreads across the receiving cells (that express the morphogen receptor, *v*), via diffusion or other forms of passive or active transport (at a rate D_u). The morphogen also decays at a constant (k_u) rate. This scheme is often called synthesis-diffusion-degradation (SDD; Wartlick, Kicheva, & Gonzalez-Gaitan, 2009). Theoretical analysis of this scenario (reviewed in Box 1) shows that, at steady state, the gradient has an exponentially decaying profile in which its characteristic length ("λ") is proportional to (the square root of) the ratio between the effective diffusion D_u and degradation constant k_u of the morphogen (as in Eq. 9). In Fig. 2 we show that the experimentally determined Hh gradients in different organs of the developing fly fit well the exponential profile predicted by the SSD model.

To generate a Hh-driven differentiation wave, the simplest solution would be to couple cell differentiation to the increase in the characteristic length λ that the gradient experiences as it evolves toward the steady state. Using experimentally determined values for D_u and k_u (Fried et

Box 1. Synthesis-diffusion-degradation theory of morphogen gradients.

How morphogenetic molecules adjust to establish gradients of different length to drive patterning of tissues of different sizes is still not well understood. Here, we review the features that shape a morphogen gradient in the context of the synthesis-diffusion-degradation scenario (SDD) (Rogers & Schier, 2011; Wartlick et al., 2009), where a given molecule is produced at one specific region of the system, spreads and gets degraded at a constant rate. The Reaction-Diffusion partial differential equations that describe the dynamics of the system can be derived based on mass action kinetics with the general form:

$$\frac{\partial u(x,t)}{\partial t} = D_u \frac{\partial^2 u(x,t)}{\partial x^2} - k_u \cdot u(x,t) \tag{1}$$

The diffusion term is simply derived from Fick's second law, where D_u represents an *effective* diffusion constant. The degradation term is defined as a simple linear dependence on the morphogen concentration with rate k_u. Eq. (1) has a steady state solution $u_{ss}(x)$ where the second spatial derivative of u is proportional to itself.

$$\frac{\partial^2 u_{ss}(x)}{\partial x^2} = \frac{k}{D} u_{ss}(x) \tag{2}$$

Since exponential functions have the unique property of their derivatives being proportional to the function itself, a general solution for u takes the form:

$$u_{ss}(x) = A \cdot e^{-x/\lambda} + B \cdot e^{+x/\lambda} \tag{3}$$

The boundary conditions are used to determine the integration constants A and B. Since we are interested in a typical morphogen gradient that is being continuously produced at one edge of the system, the first boundary condition is defined as $u_{ss}(0) = u_0$.

$$u_{ss}(0) = A \cdot e^{-0/\lambda} + B \cdot e^{+0/\lambda} = A + B = u_0 \tag{4}$$

On the other hand, if the dimensions of the system are sufficiently large compared to the characteristic length λ of the exponential, we can define the concentration of the morphogen as zero at the opposite edge of the system ($u_{ss}(L) = 0$). Therefore,

$$u_{ss}(L) = A \cdot e^{-L/\lambda} + B \cdot e^{+L/\lambda} = 0 \tag{5}$$

Since the second term of Eq. (5) increases when x increases (i.e., we move away from the morphogen source), B has to be zero. This way, $A = u_0$ and the solu-

tion has the form a single exponential:

$$u_{ss}(x) = u_0 \cdot e^{-x/\lambda} \tag{6}$$

To study the explicit dependence of the characteristic length λ on the parameters of the reaction, we take the second derivative of Eq. (6):

$$\frac{\partial^2 u_{ss}(x)}{\partial^2 x} = \frac{1}{\lambda^2}\left(u_0 \cdot e^{-x/\lambda}\right) = \frac{u_{ss}}{\lambda^2} \tag{7}$$

This expression is then substituted into the steady state solution in Eq. (2)

$$\frac{u_{ss}(x)}{\lambda^2} = \frac{k_u}{D_u} u_{ss}(x) \tag{8}$$

Therefore, λ depends directly on the diffusion and degradation of the morphogen as

$$\lambda = \sqrt{\frac{D_u}{k_u}} \tag{9}$$

The previous equation represents the analytical solution to the synthesis-diffusion-degradation (SDD) interaction scheme, and shows that the distance that the morphogen travels results from the balance between its effective diffusion coefficient and its degradation rate.

al., 2016) and solving Eq. (1) numerically, the time-evolution of the gradient shows that the dynamics of λ is fast (lines in Fig. 4A) and the steady state is reached in about 30 min (dots in Fig. 4A). This dynamics is much faster than the actual OC differentiation, which occurs in the order of days (Garcia-Morales et al., 2019), indicating that coupling between diffusion/degradation and cell differentiation is unlikely as a wave-generating mechanism.

Another strategy would be to modify directly some of the three major parameters of the SDD: the rates of morphogen synthesis, diffusion and degradation. The concentration of ligand calculated by SDD with measured D_u and k_u (Fried et al., 2016), and amplitude at the source "u_0" for Hh (Garcia-Morales et al., 2019), falls below 10% of its maximal value well before the 50 μm width of the ocellus. If we use this 10% as an arbitrary minimum for an effective Hh signaling, can changes in synthesis, diffusion or degradation during OC differentiation make the gradient reach farther? In Fig. 4B we show that, to reach the

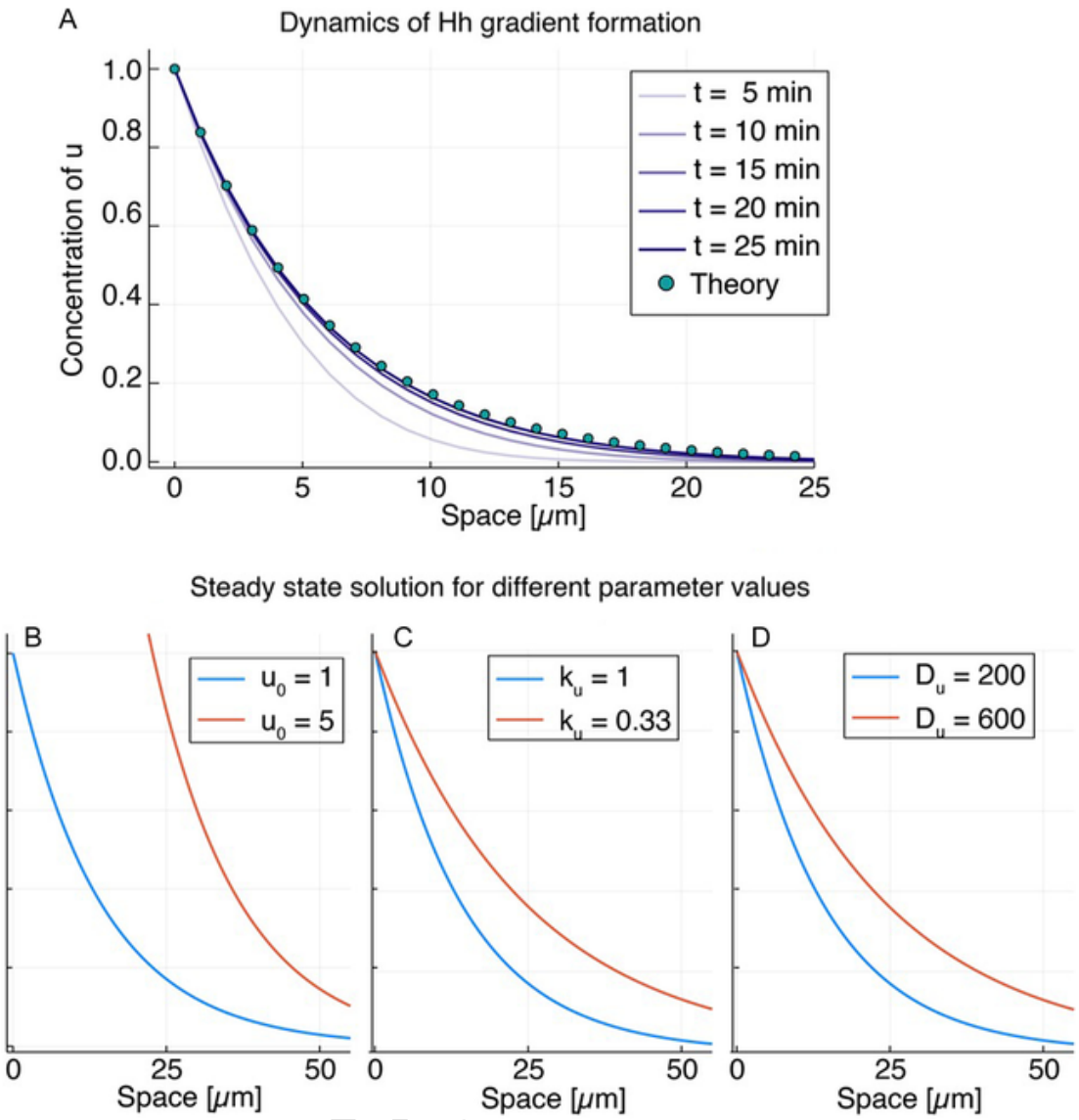

Fig. 4. Dynamics of Hh gradient formation. (A) Time evolution of the gradient profile in the SDD approach (reviewed in Box 1) using values of the effective diffusion (D_u = 118 μm^2 × h^{-1}) and effective degradation (k_u = 3,6 h^{-1}) obtained from Fried et al. (2016). Each line corresponds to the profile every 5 min. The steady state profile predicted for these parameter values is plotted as dots. (B–D) Changes in the steady state profile when different parameters are modified to obtain an amount of *u* at the end of the region of at least a 10% value of the amplitude at the source: (B) rate of production, (C) effective diffusion or (D) effective degradation. Other parameters are chosen to fit the experimental gradients measured in Fig. 2.

end of the ocellus with concentrations of morphogen above 10%, the concentration of Hh at the source should increase at least five times. This is a large increase. And even if this was the strategy used in other organs, the measured trend in the ocellus is the opposite, with Hh maximal amplitude decreasing over developmental time (Garcia-Morales et al., 2019).

Modulation of the diffusion and/or degradation rates is yet another possibility. In fact, it has been shown that changes in the composition of the extracellular matrix proteoglycans, or in the morphogen degradation rates during development affect the signaling gradient of Hh, Wg/Wnt-1 or Dpp/BMP-2 (Akiyama et al., 2008; Neto, Aguilar-Hidalgo, & Casares, 2016; Rogers & Schier, 2011; Wartlick et al., 2009, 2011). We explored the impact of these variations (Fig. 4C and D): obtaining Hh concentrations above 10% maximal across the whole ocellus requires variations in k_u or D_u of at least three times. These are again large changes in rate constants.

So far, we have not made explicit a major biochemical step that shapes morphogen gradients: the interaction of the ligand with its receptor. This step has been shown to be of key relevance in the establishment of the Hh gradient, as the interaction with its receptor Ptc restricts Hh's mobility and availability (Briscoe, Chen, Jessell, & Struhl, 2001; Chen & Struhl, 1996). In Box 2, we expand the theoretical analysis of the SDD model by including the binding/unbinding of u and v and the clearance/inactivation of the ligand:receptor complex uv (by, for example, endocytosis), and shown schematically in Fig. 5A.

After making some basic assumptions, the system of equations can be reduced and solved analytically, and the resulting morphogen profile is again an exponentially decaying gradient (Eq. 24). Now, the characteristic length depends on the parameters describing the ligand:receptor interaction and, more importantly, on the relative amounts of receptors available for binding (Eq. 24). Fig. 5B shows the steady state solution of Eq. (23) for different receptor concentrations v_0, keeping all other variables unchanged. If the concentration of free receptor is reduced, the length of the gradient increases significantly (Fig. 5B).

For instance, a simple scenario of reduced free receptor is illustrated (Fig. 5C–E) using numerical simulations for the interactions between ligand and receptor in a spatial system. In the absence of saturation (Fig. 5C), the gradient is short and reaches a steady state in just 5 hours. However, when the amount of available receptor is limited by a strong and stable interaction with the ligand (Fig. 5D), the gradient moves further away from the source. This saturation effect is best observed in Fig. 5E, that shows that the majority of receptors are bound to u forming a complex uv, allowing the further spread of the ligand u.

Box 2. Synthesis-diffusion-degradation-clearance theory of morphogen gradients.

The interaction of the diffusive ligand with its receptor can also affect the shape and reach of a morphogen gradient. This system can be also described in terms of partial differential equations based on mass action kinetics:

$$\frac{\partial u(x,t)}{\partial t} = D_u \frac{\partial^2 u(x,t)}{\partial x^2} - k_u \cdot u(x,t) + k_{off} \cdot uv(x,t) - k_{on} \cdot u(x,t) \cdot u(x,t) \tag{10}$$

$$\frac{\partial uv(x,t)}{\partial t} = D_{uv} \frac{\partial^2 uv(x,t)}{\partial x^2} - k_{uv} \cdot uv(x,t) - k_{off} \cdot uv(x,t) + k_{on} \cdot u(x,t) \cdot v(x,t) \tag{11}$$

$$\frac{\partial v(x,t)}{\partial t} = D_v \frac{\partial^2 v(x,t)}{\partial x^2} - k_v \cdot v(x,t) + k_{off} \cdot uv(x,t) - k_{on} \cdot u(x,t) \cdot v(x,t) \tag{12}$$

where u, v and uv refer to the concentration of ligand, receptor and ligand-receptor complex. Constants k_{on} and k_{off} correspond to the affinity and dissociation rates of the interaction between ligand and receptor. Similarly, D_u, D_v and D_{uv} are the diffusion constants, and k_u, k_v and k_{uv} are the clearance rate constants of u, v and uv. The condition for the conservation of mass of the morphogen is:

$$u_{total}(x,t) = u(x,t) + uv(x,t) \tag{13}$$

and the derivative of the last expression is simply:

$$\frac{\partial u_{total}(x,t)}{\partial t} = \frac{\partial u(x,t)}{\partial t} + \frac{\partial uv(x,t)}{\partial t} \tag{14}$$

The change of u_{total} is now written in terms of the change of the two forms of u:

$$\frac{\partial u_{total}(x,t)}{\partial t} = Du \frac{\partial^2 u(x,t)}{\partial x^2} - k_u \cdot u(x,t) + D_{uv} \frac{\partial^2 uv(x,t)}{\partial x^2} - k_{uv} \cdot uv(x,t) \tag{15}$$

As a first approximation, we will assume that the kinetics of binding and dissociation are fast (normally in the order of seconds) compared to the diffusion and degradation rates of the morphogen (normally in the order of minutes). This allows us to separate the two time scales and assume that there is a local equilibrium at all times between u and uv. In this condition, the ratio between the two forms of the ligand at equilibrium is simply:

$$uv = \frac{k_{on}}{k_{off}} u \cdot v = \frac{u \cdot v}{k_d} \tag{16}$$

where k_d is defined as the dissociation constant of the interaction between ligand and its receptor. Using this approximation into Eq. (14) we obtain:

$$\frac{\partial u_{total}(x,t)}{\partial t} = \frac{\partial u(x,t)}{\partial t} + \frac{1}{k_d} \frac{\partial (u(x,t) \cdot v(x,t)}{\partial t} \tag{17}$$

If we assume that only a small amount of the total receptors in the system is bound to a ligand, the concentration of v can be set as constant ($v(x,t) = v_0$), and therefore, it can be taken out of the derivative.

$$\frac{\partial u_{total}(x,t)}{\partial t} = \frac{k_d + v_0}{k_d} \frac{\partial u(x,t)}{\partial t} \tag{18}$$

Next, we assume that the diffusion of the receptor v and the ligand-receptor complex uv are much slower than the diffusion rate of the free ligand u (therefore, $D_v = D_{uv} = 0$). Taking this into account, and substituting Eq. (18) into Eq. (15), we obtain:

$$\begin{aligned} \frac{k_d + v_0}{k_d} \frac{\partial u(x,t)}{\partial t} = D_u \frac{\partial^2 u(x,t)}{\partial x^2} - k_u \cdot u(x,t) \\ - k_{uv} \cdot \frac{u(x,t) \cdot v_0}{k_d} \end{aligned} \tag{19}$$

and rearranging terms becomes:

$$\begin{aligned} \frac{\partial u(x,t)}{\partial t} = \frac{D \cdot k_d}{k_d + v_0} \frac{\partial^2 u(x,t)}{\partial x^2} \\ - \frac{k_d}{k_d + v_0} \left(k + \frac{k_{uv} \cdot v_0}{k_d} \right) \cdot u(x,t) \end{aligned} \tag{20}$$

Due to similitude with Eq. (1), we define the effective diffusion and degradation rate constants as:

$$D_{eff} = \frac{D \cdot k_d}{k_d + v_0} \tag{21}$$

$$k_{eff} = \frac{k_d}{k_d + v_0} \left(k + \frac{k_{uv} \cdot v_0}{k_d} \right) \tag{22}$$

Therefore, Eq. (20) can be rewritten simply as:

$$\frac{\partial u(x,t)}{\partial t} = D_{eff}\frac{\partial^2 u(x,t)}{\partial x^2} - k_{eff}\cdot u(x,t) \tag{23}$$

which can be solved analytically following the same strategy as Eq. (1) with the same solution (Eq. 6). The characteristic length of the exponential profile is given by Eq. (9), so substituting the expressions for effective diffusion and degradation rates (Eqs. 21 and 22), we obtain

$$\lambda = \sqrt{\frac{D_{eff}}{k_{eff}}} = \sqrt{\frac{D}{\left(k + \frac{k_{uv}\cdot v_0}{k_d}\right)}} \tag{24}$$

This equation shows that now the average distance traveled by a morphogen ligand increases when the concentration of its receptor decreases.

To analyze whether this receptor saturation is seen *in vivo*, we measured the colocalization of Hh and Ptc in the ocelli, in larvae expressing fluorescently tagged Hh (GFP:Hh) and Ptc (RFP:Ptc) at endogenous levels (Chen et al., 2017). The results in Fig. 3E show that a large fraction of Ptc colocalizes with Hh. More importantly, this percentage is maintained all along the gradient (i.e., in both high and low Hh concentrations), suggesting that indeed the receptor Ptc is saturated throughout the tissue. Another important observation is that now the predicted dynamics of the gradient spreading in much slower and closer to the timing of ocellar differentiation (about 50 h).

A side effect of the receptor saturation is that the gradient changes from exponential to a more linear profile (Fig. 5D). This change is consistent with experimental observations in the Drosophila ocelli (Garcia-Morales et al., 2019), where the Hh profile becomes more linear as differentiation takes place.

The same effective reduction of available free receptor can be achieved if the rate of receptor transcription is much slower relative to the clearance rate of the bound receptor, which can be safely assumed to be the case. This scenario was simulated in Fig. 5F–H, where we compare the profile dynamics when the transcription and clearance rates are of the same scale (Fig. 5F) with when the production is slower (similar equilibrium concentration of *v*: Fig. 5G). In the latter, again the gradient extends farther and becomes more linear. The progressive re-

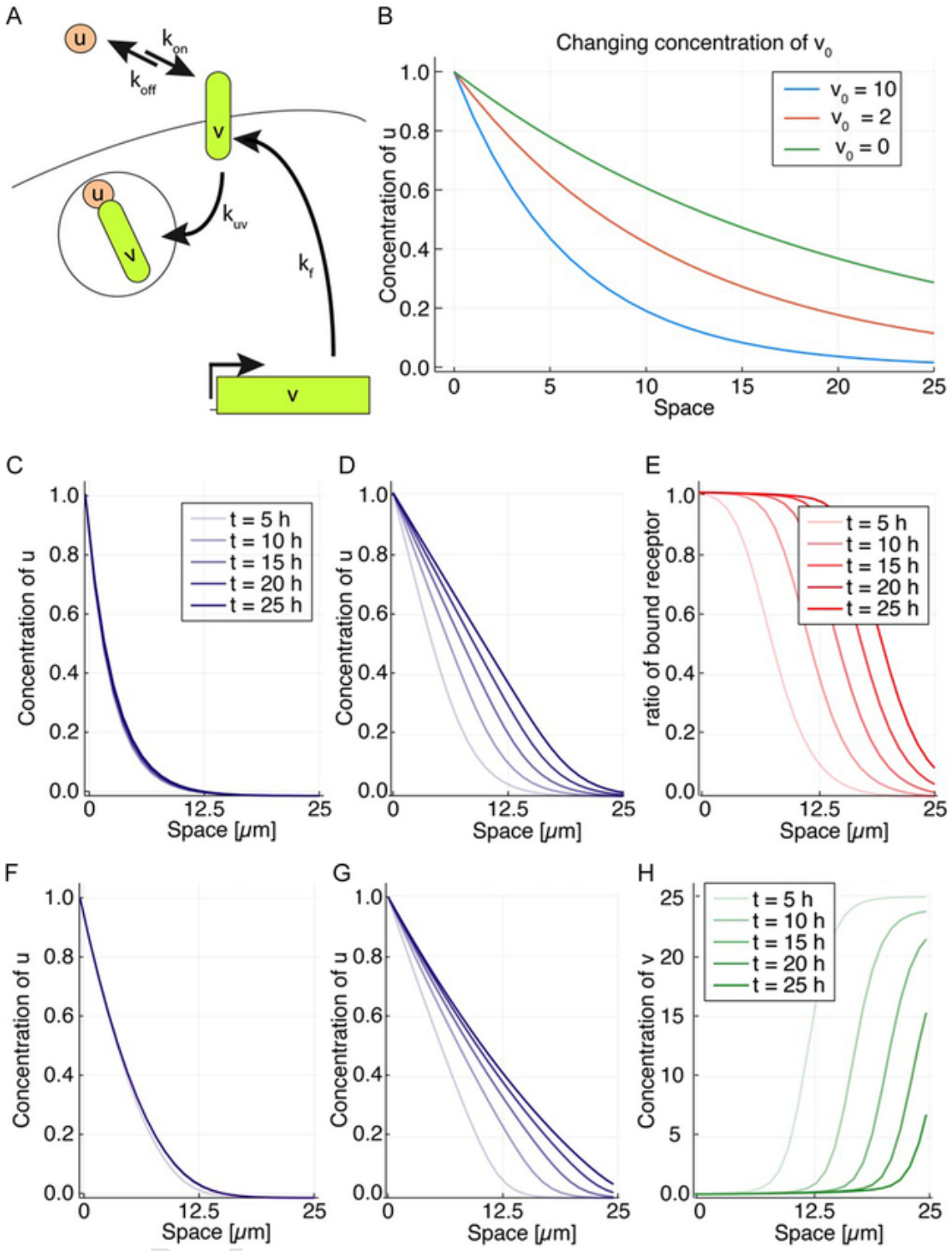

Fig. 5. Reduction in the concentration of receptor extends the characteristic length of the gradient. (A) Scheme of the interaction between ligand (*u*) and receptor (*v*) molecules, with the active complex *uv* being internalized and cleared. (B) Theoretical prediction of the changes in the gradient with the value of receptor v_0. (C–E) Comparison of gradient dynamics in conditions of (C) no receptor saturation and (D) receptor saturation. (E) Ratio of bound *uv* versus unbound *v* in conditions of receptor saturation. (F–H) Comparison of gradient dynamics in conditions of fast (F) and slow (G) rate of *v* production. (H) Spatial profile of free receptor *v* at different time points in conditions of slow rate of production.

duction of free receptor is clearly shown in Fig. 5H as the ligand spreads in space. Comparison between the lines that illustrate the gradient at different time points (Fig. 5D and G), shows that the profile keeps advancing at a progressively decreasing speed. Therefore, the same 10% threshold for the morphogen concentration used above would be eventually reached if the simulation were allowed to run for a longer time.

7. WHEN A NEGATIVE FEEDBACK "LOG TRANSFORMS" THE GRADIENT

It has recently been shown that, indeed, as the ocellar precursor cells differentiate as PRs, the Ptc receptor is transcriptionally repressed (Garcia-Morales et al., 2019). Cells closest to the source are the first to differentiate and to downregulate Ptc. As a consequence, these PRs cells no longer bind and consume Hh, and so the free morphogen travels further, triggering differentiation in adjacent cells, with the process propagating away from the source. To illustrate the effect of this feedback repression of the receptor v, we define a set of coupled partial differential equations for ligand u, receptor v and ligand:receptor complex uv, where the expression of v is modulated by the active uv complex following a Hill function.

Again, only free u is allowed to disperse and is degraded at a rate k_u. In addition, u binds v and the uv complex is cleared with a constant k_{uv}. A scheme showing these interactions is shown in Fig. 6A. Numerical solution of the equations either in the absence (Fig. 6B) or in the presence (Fig. 6C) of the negative feedback is shown for different time points.

The introduction of the feedback produces three major changes in the gradient dynamics: its characteristic length is longer (i.e., the gradient stretches farther); the steady state is reached more slowly due to the dynamic coupling between differentiation time (that represses v) and the gradient expansion; and the shape of the gradient is changed—no longer exponential but approaching linearity. A more complete two-dimensional model has been presented in Garcia-Morales et al. (2019).

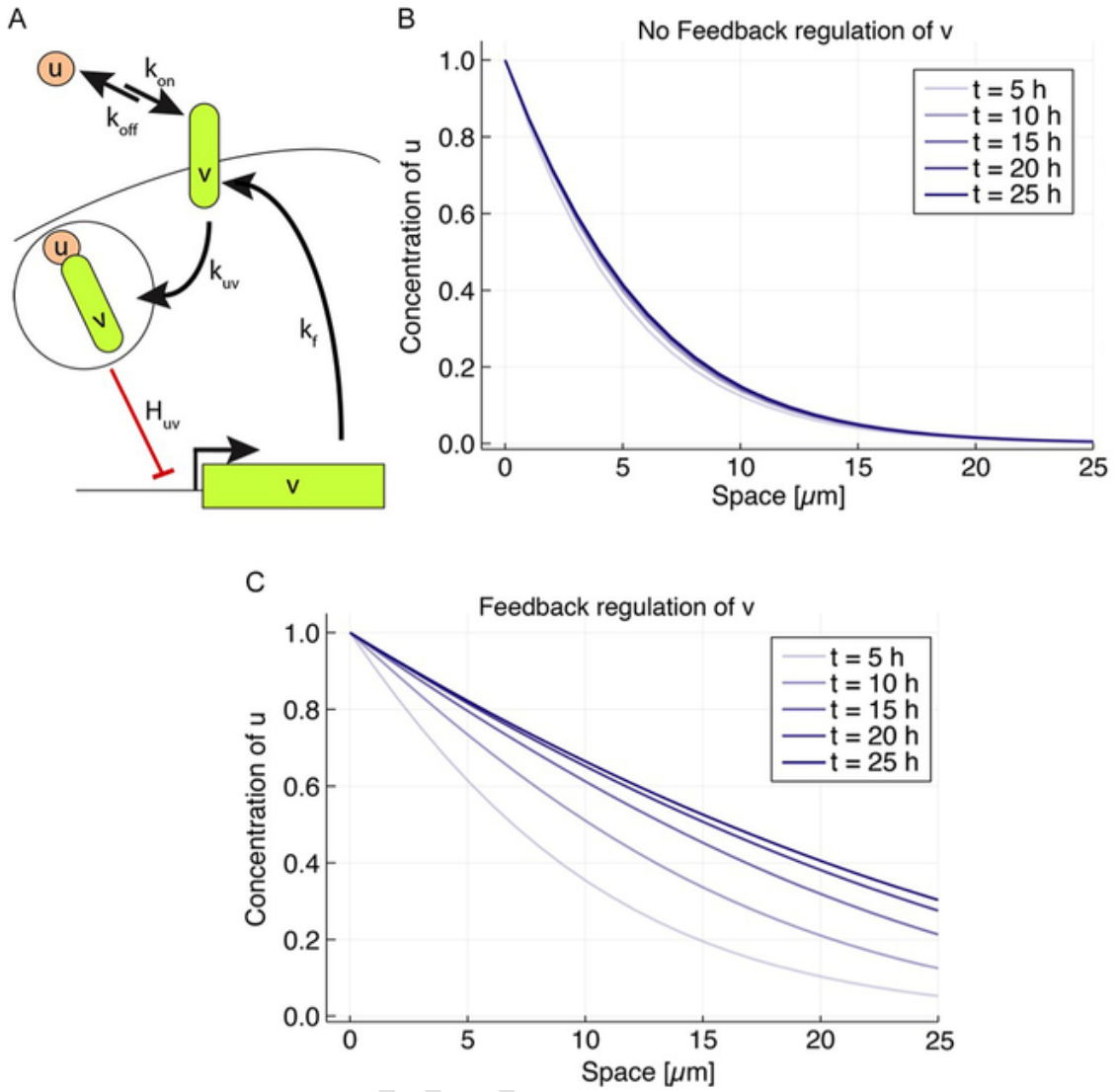

Fig. 6. Feedback loop in the concentration of receptor shapes the gradient dynamics. (A) Scheme of the interaction between ligand and receptor molecules, with the active complex *uv* being internalized and driving repression of the production of free receptor. (B) Numerical simulations of the gradient profile with no feedback interaction. (C) Numerical simulations of the system with the same parameter values, but including feedback repression of the receptor *v*.

8. A STATIC MORPHOGEN SOURCE WITH A DYNAMIC SIGNALING WORKS LIKE A DEVELOPMENTAL METRONOME

By making the regulation of Hh depend on PR differentiation, the gradient experiences a dynamic change that occurs at the same rate as that of cell differentiation. Because the resulting dynamics linearizes the signaling output in space, Hh-induced PR differentiation occurs at a

constant pace. In addition, colocalization studies suggest that the receptor Ptc is likely saturated (Fig. 3), which can also contribute to the linearization of the gradient, as shown in the previous sections (Fig. 5). This linearization is equivalent to a mathematical "log-transform." The morphogen gradient, this time, is not used to specify different cell types in space, as the OC retinas are composed by a single PR type all throughout, but to generate a wave of differentiation (Garcia-Morales et al., 2019). Rather than specifying space, Hh "marks a pace." It is important to note that even though the regulation of receptor expression occurs at the single-cell level, the "log-transform" operation emerges across a field of cells.

But how is this system expected to perform in the face of the inescapable biochemical noise? One potential problem might arise if the receptor Ptc had low occupancy, as this would increase binding noise (Lander, 2013). However, as mentioned above, Ptc is likely saturated along the whole signaling range, which would minimize this sensitivity. Ptc saturation, though, could in turn increase the sensitivity of the system to fluctuations in Hh production rate, unless signal measurements were carried out before the gradient reaches steady state (Lander, 2013). In fact, and as we mentioned above, the Hh gradient is not in steady state in the OC (Garcia-Morales et al., 2019). Then, the downregulation of the Ptc receptor as cells differentiate, generates an internal biochemical clock that, when linked to the dynamic Hh gradient, results in an increased resistance to fluctuations in Hh concentration (Garcia-Morales et al., 2019).

9. INTRINSIC CONSTRAINTS TO THE VARIATION OF OCELLAR SIZE IMPOSED BY THE GRADIENT

The patterning of the small eyes of flies is controlled by a dynamic (in space and time) gradient of Hh produced from a spatially fixed source. We have argued above that the reach of such a gradient is limited, unless some of its biochemical constants or the availability of the receptor change dramatically. Do these limitations set a maximum size for the ocelli? The range of sizes between different fly species is enormous, spanning two orders of magnitude in body length: from 0,5 mm of some Phorid flies to the 70 mm of *Gauromydas heros*. If all these flies used a Hh gradient to control the size and pattern of their

ocelli similar to the one described in *Drosophila*, we would expect that the size of their ocelli would not scale perfectly with body size—that is, ocelli should be disproportionally smaller in large flies when compared to smaller species. This seems to be the case. In Fig. 7A the wing length (a correlate of body size) and the ocellar size (measured as the length of the major axis of the elliptical lens of the ocellus) of a small (*Drosophila melanogaster*) and a large fly (*Episyrphus balteatus*) are compared. While *Episyrphus* wings are four times longer, its ocelli are

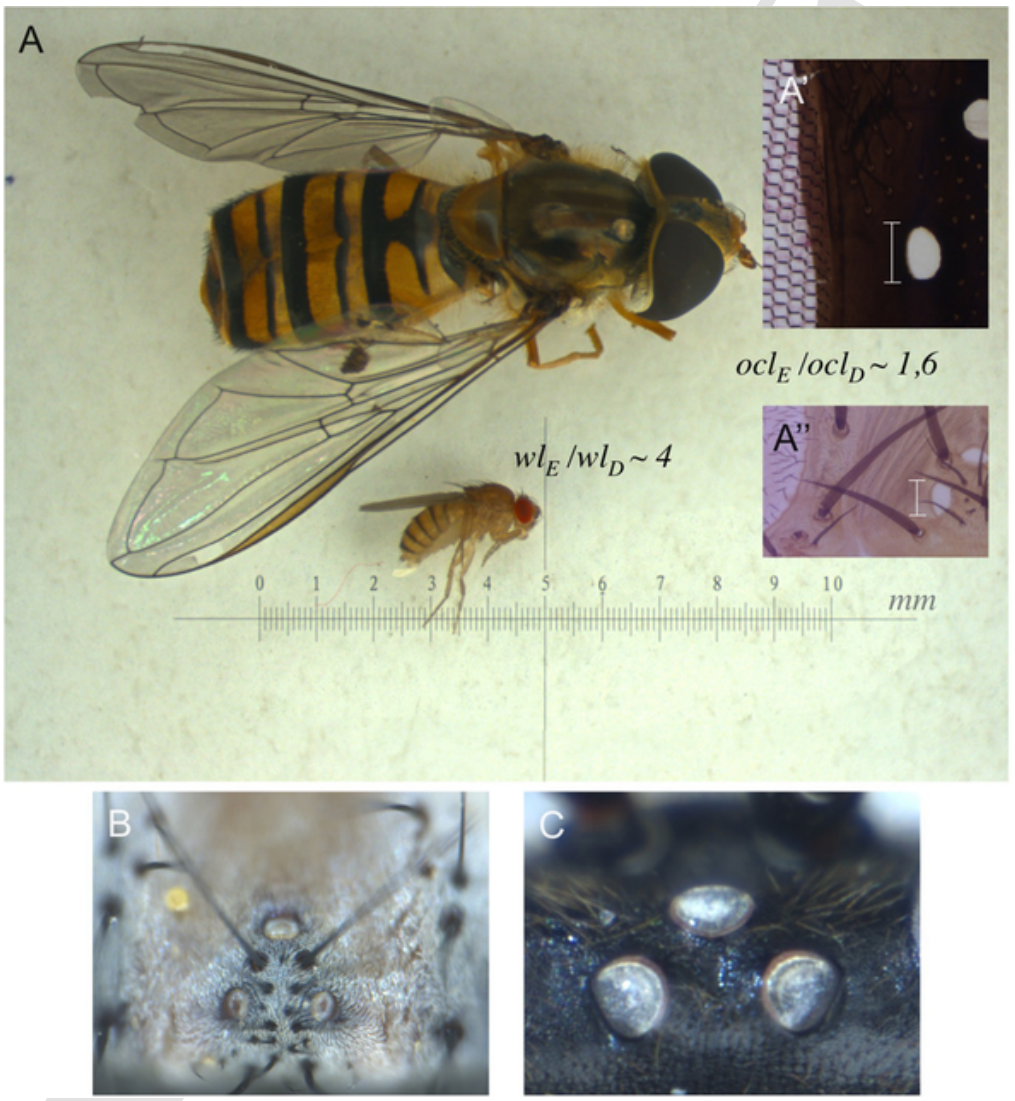

Fig. 7. Ocellar size in different species in relation to body size. (A) A large fly (top, *Episyrphus balteatus*) and a small fly (bottom, *Drosophila melanogaster*). The ratio of their wing length is indicated (*wl;* the wing length is a correlate of body size). Microscopic images of the adult ocelli of *Episyrphus* (A′) and *Drosophila* (A″) at the same magnification. The relative width of their posterior ocelli (*ocl*) is indicated. (B, C) Ocelli of the fly *Senotainia tricuspis* (NHMUK010579737) (Sarcophagidae) (B) and the wasp *Dusona bicoloripes* (NHMUK010579721) (Ichneumonidae) (C) at the same magnification, showing the much larger ocelli of the wasp.

only ~ 1,6 times the width of *Drosophila*'s. Of course, this limit in ocellar size might be the result of natural selection: above a certain size, there might not be a selective advantage in having larger ocelli. However, very large ocelli are present in other insect groups, such as Odonata (dragonflies and damselflies) and Hymenoptera (wasps and bees) (Berry, Stange, & Warrant, 2007; Ribi, Warrant, & Zeil, 2011) (see also Fig. 7B and C). Therefore, it is possible that, indeed, ocellar size in flies is limited by the effective range of Hh action, as suggested previously (Aguilar-Hidalgo, Becerra-Alonso, Garcia-Morales, & Casares, 2016; Aguilar-Hidalgo et al., 2013). Ocelli larger than those of Diptera might need different mechanisms, although surely based on Hh, to be patterned.

10. CONCLUDING REMARKS

In this review, and using as motivation the role played by Hh in the differentiation of the *Drosophila* eyes, we have explored how a morphogen gradient can stretch itself to pattern tissues of different size. In *Drosophila*, when the eye is larger than a certain size, new mechanisms come into place to overcome these limitations. Finally, we note that PR differentiation in both the small and the large eyes of flies proceeds at a constant pace, despite their using different regulatory mechanisms to achieve this linearity. In the case of the OC, perhaps the functional need of generating sufficiently large retinas resulted in the selection of subtle changes in the regulatory network that allowed the extension of the gradient reach without the need of more dramatic or pleiotropic modifications affecting, for example, the diffusivity or degradation of the morphogen itself. Here, we propose three different strategies: saturation, slow transcription (relative to diffusion) or down-regulation of the receptor. In the particular case of the OC, we observe experimental evidence of the three, so maybe the system uses a combination of these strategies. As we have shown, this extension brings about immediately the linearization of the gradient which, in turn, can be used to induce differentiation at a constant pace. The CE, being larger, requires the introduction of at least one extra link within the PR regulatory network: the production of Hh itself by PRs. Still, a detailed study of Hh distribution and Ptc dynamics anterior to the differentiation wave in the CE is lacking, so it is not yet known whether Hh signaling

in the CE is further modified using some of the strategies used in the OC.

In any case, why should PR differentiation proceed at a constant pace? Recent studies show how signal transduction through highly non-linear biochemical pathways often results in linear outputs (Goentoro & Kirschner, 2009; Nunns & Goentoro, 2018). This linearity in signal transduction increases the fidelity of the signaling. We suggest that linearity of patterning processes allows the uniform deployment of these processes throughout development, allowing an easier control. For example, the control of a process whose rate varies with developmental time may require also varying the intensity of the control mechanism as time passes (that is, *developmental time* becomes an additional variable), while a linear process may be controlled even when the perturbation has already happened. Also, a linear process is less prone to amplify or attenuate changes in the input signal. Finally, the coupling or coordination between developmental processes might be facilitated if these processes develop at constant speeds.

11. MATERIALS AND METHODS

Codes "NHMUK" are specimen codes of the Natural History Museum, London (UK) collection. The results presented in Figs. 1–3 were obtained using methods described in Garcia-Morales et al. (2019), except for colocalization studies of Hh:GFP and Ptc:GFP. For this analysis, eye-antennal discs of Hh:GFP/CyO; Ptc:RFP larvae (Chen et al., 2017) were dissected and stained with anti-GFP, anti-RFP and anti-Eya (this latter to label the OC-competent region) as in Garcia-Morales et al. (2019) and imaged under a Zeiss LSM880 Airyscan. Images were processed with Softworx Suite 2.0 (Applied Precision) and analyzed with Imaris (Bitplane). Punctate signal ("vesicles") in the red and green channels was selected with the function "slice." Only vesicles with diameters equal or larger than 0,5 μm were considered in order to minimize noise inclusion. The "spots" function was used to select the vesicles of the defined diameter and the "spots colocalize" function to identify those where the two signals overlapped. The three signals (green, red and yellow ("colocalized")) were represented in 3D with the "vantage plot" function and collapsed into 2D for data representation using bins of 0,05 μm. The data shown here is representative of six samples.

ACKNOWLEDGMENTS AND FUNDING

F.C. is funded through grants BFU2015-66040-P, PGC2018-093704-B-I00 and MDM-2016-0687, and D.G.M. through grants BFU2014-53299-P and RTI2018-096953-B-I00, all from Ministerio de Ciencia, Innovación y Universidades of Spain. A SYNTHESYS grant (GB-TAF 5341) allowed F.C. to visit the Natural History Museum (London, UK) to study and image the ocellar complex across a large sample of Diptera species (and some hymenoptera). F.C. thanks the collaboration of Daniel Whitmore and the help of Vladimir Blagoderov and Benjamin Price.

REFERENCES

Aguilar-Hidalgo, D., Becerra-Alonso, D., Garcia-Morales, D., Casares, F., 2016. Toward a study of gene regulatory constraints to morphological evolution of the Drosophila ocellar region. Development Genes and Evolution 226, 221–233.

Aguilar-Hidalgo, D., Casares, F., Lemos, M.C., 2018. Patterning, dynamics and evolution in the ocellar complex of the fruit fly. In: Archilla, J.F.R., Palmero, F., Lemos, M.C., Sanchez-Rey, B., Casado-Pascual, J. (Eds.), Nonlinear systems. Nonlinear phenomena in biology, optics and condensed matter. Springer International Publishing, Cham, Switzerland, pp. 39–62.

Aguilar-Hidalgo, D., Dominguez-Cejudo, M.A., Amore, G., Brockmann, A., Lemos, M.C., Cordoba, A., et al., 2013. A Hh-driven gene network controls specification, pattern and size of the Drosophila simple eyes. Development 140, 82–92.

Akiyama, T., Kamimura, K., Firkus, C., Takeo, S., Shimmi, O., Nakato, H., 2008. Dally regulates Dpp morphogen gradient formation by stabilizing Dpp on the cell surface. Developmental Biology 313, 408–419.

Alexandre, C., Jacinto, A., Ingham, P.W., 1996. Transcriptional activation of hedgehog target genes in Drosophila is mediated directly by the cubitus interruptus protein, a member of the GLI family of zinc finger DNA-binding proteins. Genes & Development 10, 2003–2013.

Amore, G., Casares, F., 2010. Size matters: The contribution of cell proliferation to the progression of the specification Drosophila eye gene regulatory network. Developmental Biology 344, 569–577.

Baker, N.E., Bhattacharya, A., Firth, L.C., 2009. Regulation of Hh signal transduction as Drosophila eye differentiation progresses. Developmental Biology 335, 356–366.

Berry, R.P., Stange, G., Warrant, E.J., 2007. Form vision in the insect dorsal ocelli: An anatomical and optical analysis of the dragonfly median ocellus. Vision Research 47, 1394–1409.

Blanco, J., Pauli, T., Seimiya, M., Udolph, G., Gehring, W.J., 2010. Genetic interactions of eyes absent, twin of eyeless and orthodenticle regulate sine oculis expression during ocellar development in Drosophila. Developmental Biology 344, 1088–1099.

Blanco, J., Seimiya, M., Pauli, T., Reichert, H., Gehring, W.J., 2009. Wingless and Hedgehog signaling pathways regulate orthodenticle and eyes absent during ocelli development in Drosophila. Developmental Biology 329, 104–115.

Borod, E.R., Heberlein, U., 1998. Mutual regulation of decapentaplegic and hedgehog during the initiation of differentiation in the Drosophila retina. Developmental Biology 197, 187–197.

Bras-Pereira, C., Bessa, J., Casares, F., 2006. Odd-skipped genes specify the signaling center that triggers retinogenesis in Drosophila. Development 133, 4145–4149.

Bras-Pereira, C., Potier, D., Jacobs, J., Aerts, S., Casares, F., Janody, F., 2016. dachshund potentiates hedgehog signaling during Drosophila retinogenesis. PLoS Genetics 12, e1006204.

Briscoe, J., Chen, Y., Jessell, T.M., Struhl, G., 2001. A hedgehog-insensitive form of patched provides evidence for direct long-range morphogen activity of sonic hedgehog in the neural tube. Molecular Cell 7, 1279–1291.

Brockmann, A., Dominguez-Cejudo, M.A., Amore, G., Casares, F., 2011. Regulation of ocellar specification and size by twin of eyeless and homothorax. Developmental Dynamics 240, 75–85.

Casares, F., Almudi, I., 2016. Fast and furious 800. The retinal determination gene network in Drosophila. In: Castelli-Gair Hombría, J., Bovolenta, P. (Eds.), Organogenetic gene networks. Springer, Cham, pp. 95–124.

Chen, W., Huang, H., Hatori, R., Kornberg, T.B., 2017. Essential basal cytonemes take up Hedgehog in the Drosophila wing imaginal disc. Development 144, 3134–3144.

Chen, Y., Struhl, G., 1996. Dual roles for patched in sequestering and transducing Hedgehog. Cell 87, 553–563.

Dessaud, E., Yang, L.L., Hill, K., Cox, B., Ulloa, F., Ribeiro, A., et al., 2007. Interpretation of the sonic hedgehog morphogen gradient by a temporal adaptation mechanism. Nature 450, 717–720.

Dominguez, M., 1999. Dual role for Hedgehog in the regulation of the proneural gene atonal during ommatidia development. Development 126, 2345–2353.

Dominguez, M., Brunner, M., Hafen, E., Basler, K., 1996. Sending and receiving the hedgehog signal: Control by the Drosophila Gli protein Cubitus interruptus. Science 272, 1621–1625.

Dominguez, M., Hafen, E., 1997. Hedgehog directly controls initiation and propagation of retinal differentiation in the Drosophila eye. Genes & Development 11, 3254–3264.

Dominguez-Cejudo, M.A., Casares, F., 2015. Anteroposterior patterning of Drosophila ocelli requires an anti-repressor mechanism within the hh pathway mediated by the Six3 gene Optix. Development 142, 2801–2809.

Fried, P., Sanchez-Aragon, M., Aguilar-Hidalgo, D., Lehtinen, B., Casares, F., Iber, D., 2016. A model of the spatio-temporal dynamics of Drosophila eye disc development. PLoS Computational Biology 12, e1005052.

Friedrich, M., 2006. Ancient mechanisms of visual sense organ development based on comparison of the gene networks controlling larval eye, ocellus, and compound eye specification in Drosophila. Arthropod Structure & Development 35, 357–378.

Fu, W., Baker, N.E., 2003. Deciphering synergistic and redundant roles of Hedgehog, Decapentaplegic and Delta that drive the wave of differentiation in Drosophila eye development. Development 130, 5229–5239.

Garcia-Morales, D., Navarro, T., Iannini, A., Pereira, P.S., Miguez, D.G., Casares, F., 2019. Dynamic Hh signalling can generate temporal information during tissue patterning. Development 146.

Goentoro, L., Kirschner, M.W., 2009. Evidence that fold-change, and not absolute level, of beta-catenin dictates Wnt signaling. Molecular Cell 36, 872–884.

Greenwood, S., Struhl, G., 1999. Progression of the morphogenetic furrow in the Drosophila eye: The roles of Hedgehog, Decapentaplegic and the Raf pathway. Development 126, 5795–5808.

Haynie, J.L., Bryant, P.J., 1986. Development of the eye-antenna imaginal disc and morphogenesis of the adult head in Drosophila melanogaster. The Journal of Experimental Zoology 237, 293–308.

Kicheva, A., Briscoe, J., 2015. Developmental pattern formation in phases. Trends in Cell Biology 25, 579–591.

Krapp, H.G., 2009. Ocelli. Current Biology 19, R435–R437.

Lander, A.D., 2013. How cells know where they are. Science 339, 923–927.

Ma, C., Zhou, Y., Beachy, P.A., Moses, K., 1993. The segment polarity gene hedgehog is required for progression of the morphogenetic furrow in the developing Drosophila eye. Cell 75, 927–938.

Maynard-Smith, J., Sondhi, K.C., 1960. The genetics of a pattern. Genetics 45, 1039–1050.

Mismer, D., Michael, W.M., Laverty, T.R., Rubin, G.M., 1988. Analysis of the promoter of the Rh2 opsin gene in Drosophila melanogaster. Genetics 120, 173–180.

Neto, M., Aguilar-Hidalgo, D., Casares, F., 2016. Increased avidity for Dpp/BMP2 maintains the proliferation of progenitors-like cells in the Drosophila eye. Developmental Biology 418, 98–107.

Neumann, C.J., Nuesslein-Volhard, C., 2000. Patterning of the zebrafish retina by a wave of sonic hedgehog activity. Science 289, 2137–2139.

Nunns, H., Goentoro, L., 2018. Signaling pathways as linear transmitters. eLife 7, e33617.

Pauli, T., Seimiya, M., Blanco, J., Gehring, W.J., 2005. Identification of functional sine oculis motifs in the autoregulatory element of its own gene, in the eyeless enhancer and in the signalling gene hedgehog. Development 132, 2771–2782.

Ribi, W., Warrant, E., Zeil, J., 2011. The organization of honeybee ocelli: Regional specializations and rhabdom arrangements. Arthropod Structure & Development 40, 509–520.

Rogers, E.M., Brennan, C.A., Mortimer, N.T., Cook, S., Morris, A.R., Moses, K., 2005. Pointed regulates an eye-specific transcriptional enhancer in the Drosophila hedgehog gene, which is required for the movement of the morphogenetic furrow. Development 132, 4833–4843.

Rogers, K.W., Schier, A.F., 2011. Morphogen gradients: From generation to interpretation. Annual Review of Cell and Developmental Biology 27, 377–407.

Royet, J., Finkelstein, R., 1996. hedgehog, wingless and orthodenticle specify adult head development in Drosophila. Development 122, 1849–1858.

Treisman, J.E., 2013. Retinal differentiation in Drosophila. Wiley Interdisciplinary Reviews: Developmental Biology 2, 545–557.

Viets, K., Eldred, K., Johnston Jr., R.J., 2016. Mechanisms of photoreceptor patterning in vertebrates and invertebrates. Trends in Genetics 32, 638–659.

Vollmer, J., Fried, P., Sanchez-Aragon, M., Lopes, C.S., Casares, F., Iber, D., 2016. A quantitative analysis of growth control in the Drosophila eye disc. Development 143, 1482–1490.

Wartlick, O., Kicheva, A., Gonzalez-Gaitan, M., 2009. Morphogen gradient formation. Cold Spring Harbor Perspectives in Biology 1, a001255.

Wartlick, O., Mumcu, P., Kicheva, A., Bittig, T., Seum, C., Julicher, F., et al., 2011. Dynamics of Dpp signaling and proliferation control. Science 331, 1154–1159.

Zhang, Q., Zhang, L., Wang, B., Ou, C.Y., Chien, C.T., Jiang, J., 2006. A hedgehog-induced BTB protein modulates hedgehog signaling by degrading Ci/Gli transcription factor. Developmental Cell 10, 719–729.

Keywords: *Hedgehog*; Morphogen gradient; Size; Feedback; *Drosophila*; Eye; Ocellus